Electronic Supplementary Material (ESI) for Journal of Materials Chemistry C.
This journal is © The Royal Society of Chemistry 2021

Supplementary Information

Photo- and Thermo- Salient Crystalline Hemithioindigo-Anthracene Based Isomeric Photoswitches

*Duane Hean, Luis G. Alde, Michael O. Wolf**

Department of Chemistry, University of British Columbia, 2036 Main Mall, Vancouver, British Columbia, V6T 1Z1, Canada

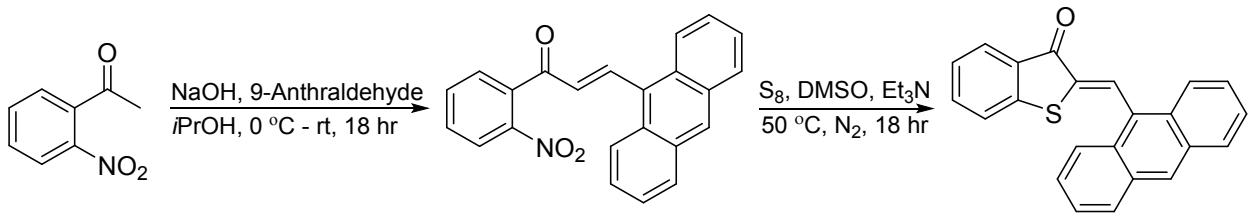

Scheme S1. Synthesis of the hemithioindigo photoswitch (*Z*)-**HTI-An**.

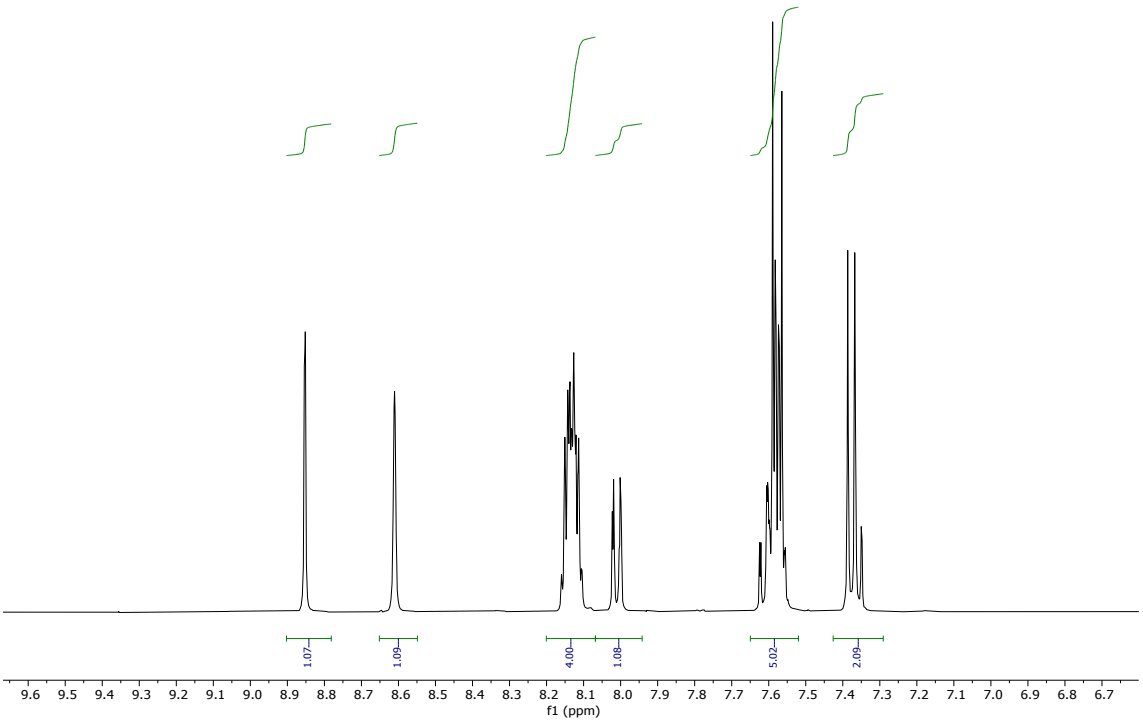

Figure S1. ^{1}H NMR (400 MHz) spectrum of (*Z*)-**HTI-An** in CD_2Cl_2.

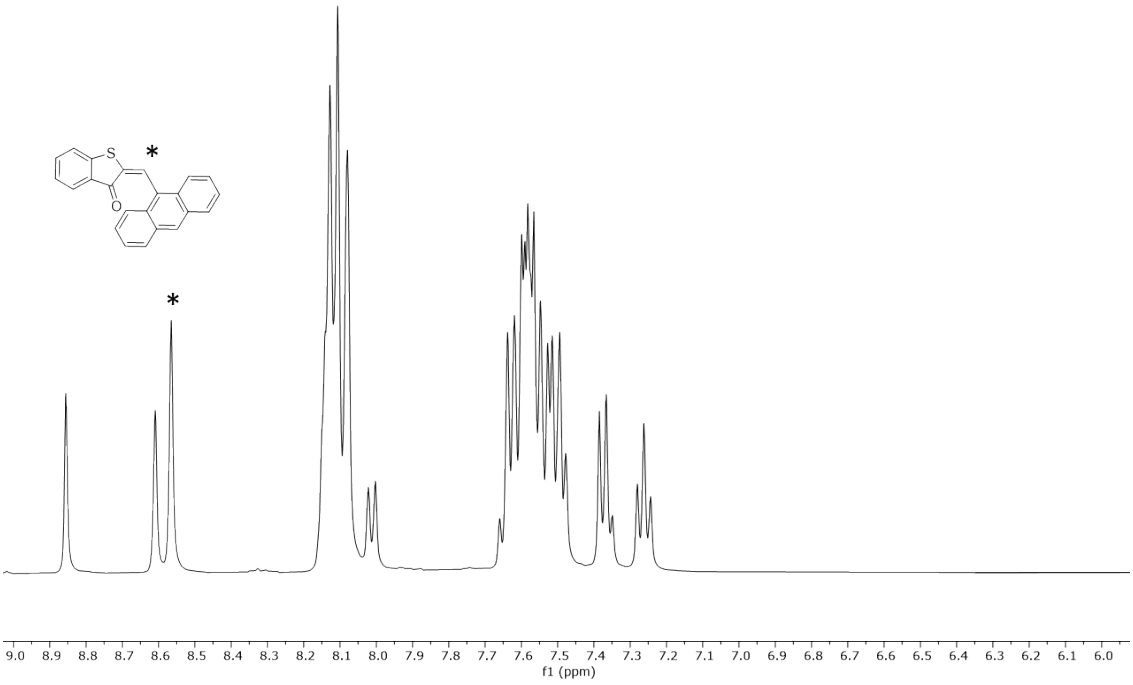

Figure S2.[1]H NMR (400 MHz) spectrum of (*E*)-**HTI-An** in CD_2Cl_2 at 80 % isomeric purity.

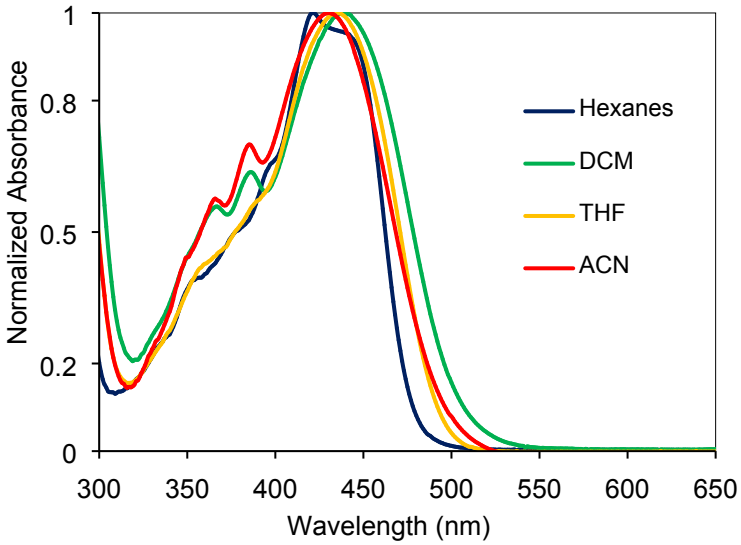

Figure S3. UV-Vis absorption spectra of (*Z*)-**HTI-An** in various solvents.

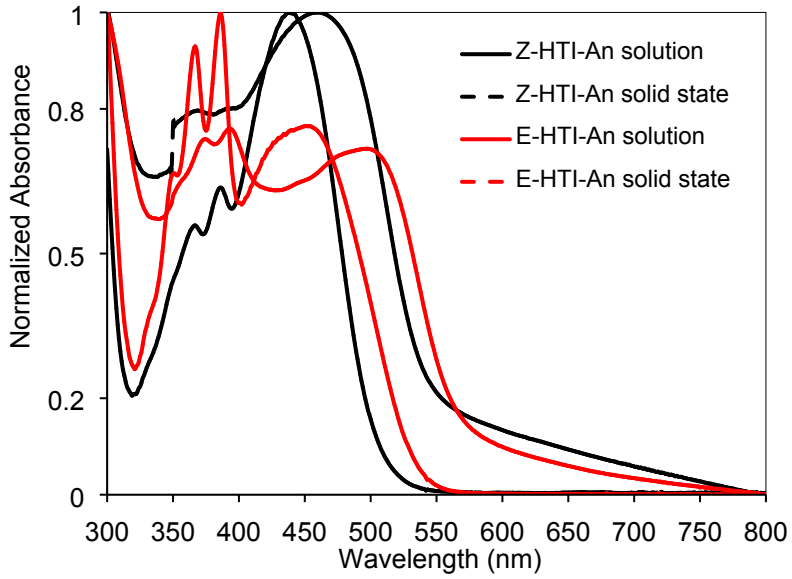

Figure S4. UV-Vis absorption spectra of solution (solid) and solid state (dashed) of (*Z*)-**HTI-An** (red) and (*E*)-**HTI-An** (black).

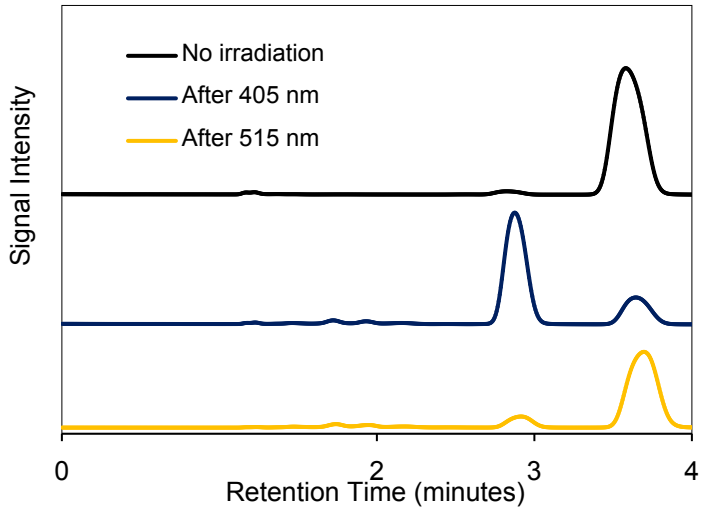

Figure S5. HPLC spectra of photo products from solution irradiation of **HTI-An**. Before irradiation the ratio was ~98 % (*Z*)-**HTI-An**, after 30 minutes of 405 nm irradiation resulting in 23 % (*Z*)-**HTI-An**: 77 % (*E*)-**HTI-An**. Following 515 nm irradiation for 30 minutes the isomerization reaction yielded 90 % (*Z*)-**HTI-An** : 10 % (*E*)-**HTI-An**.

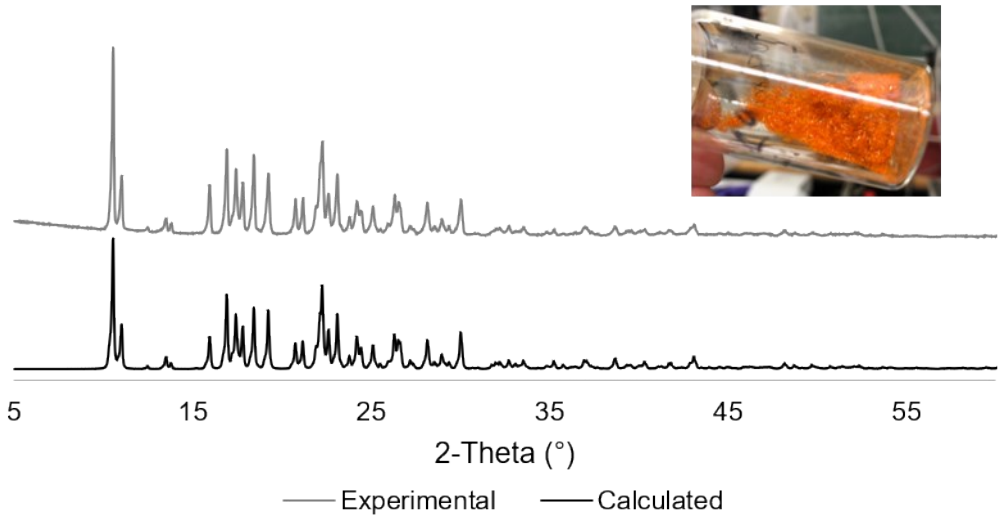

Figure S6. Comparison of the calculated (100 K) and experimental (298 K) powder X-ray diffractograms of (*Z*)-**HTI-An**. The inset is a photograph of the bulk material.

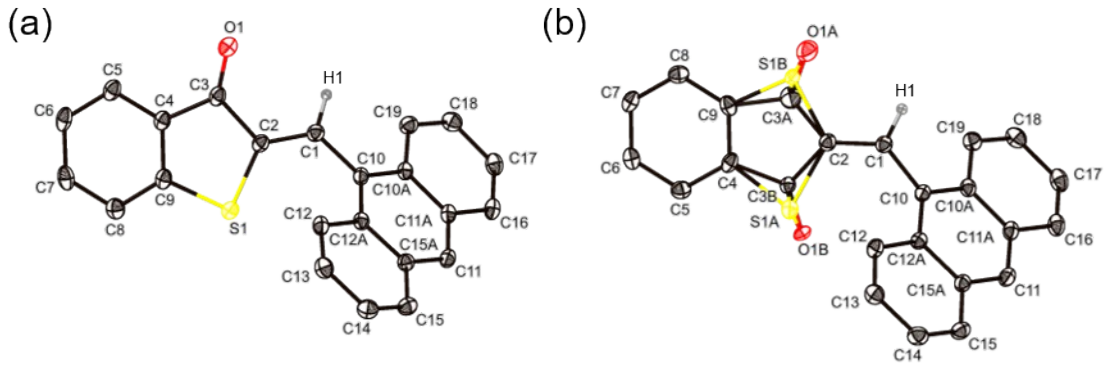

Figure S7. ORTEP diagrams of (a) (*Z*)-**HTI-An** and (b) (*E*)-**HTI-An** where ellipsoids are drawn at 50 % probability and hydrogen atoms are excluded for clarity. The site occupancy, modelled as disordered thioindigo fragments of (*E*)-**HTI-An** was determined to be 92.3: 7.7 **E** : ***Z***.

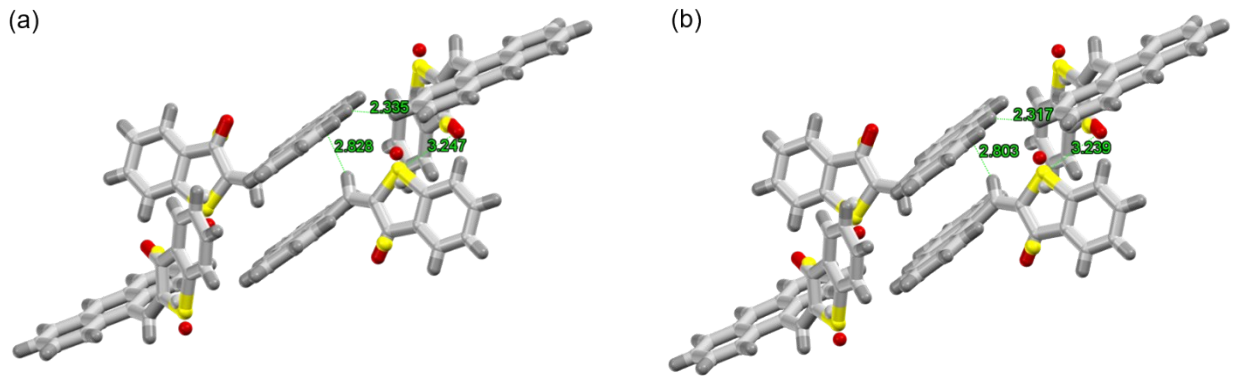

Figure S8. Short contact interactions of (a) (*E*)-**HTI-An** before irradiation and (b) (*E*)-**HTI-An** post photosalient event.

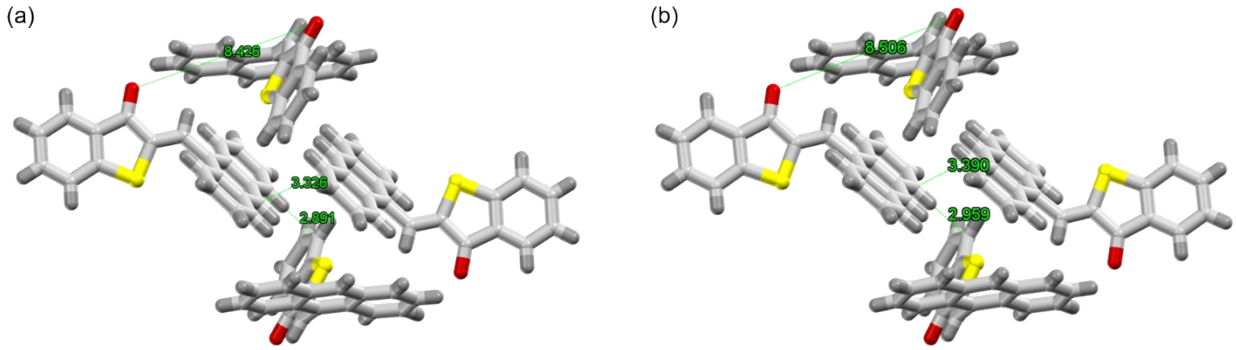

Figure S9. Short contact interactions and carbonyl oxygen distances of (a) (*Z*)-**HTI-An at** RT and (b) (*Z'*)-**HTI-An** at 400K.

Table S1. Crystal data tables of (*E*)-**HTI-An** before irradiation, post photosalient event, and after 2-hour heating.

Compound	(*E*)-**HTI-An** before irradiation	(*E*)-**HTI-An** post photosalient event	(*E*)-**HTI-An** after 2-hour heating
CCDC No.	2068879	2068880	2068881
Empirical formula	$C_{23}H_{14}OS$	$C_{23}H_{14}OS$	$C_{23}H_{14}OS$
Formula weight	338.40	338.40	338.40
Temperature/K	120	133	100
Crystal system	monoclinic	monoclinic	monoclinic

Space group	$P2_1/c$	$P2_1/c$	$P2_1/c$
a/Å	10.4430(4)	10.351(12)	10.453(3)
b/Å	13.9757(5)	13.886(17)	13.935(4)
c/Å	11.2410(4)	11.185(13)	11.229(3)
α/°	90	90	90
β/°	102.9160(10)	102.99(3)	102.990(8)
γ/°	90	90	90
Volume/Å^3	1599.09(10)	1567(3)	1593.9(8)
Z	4	4	4
ρ_{calc}g/cm^3	1.406	1.435	1.410
μ/mm^{-1}	0.210	0.214	0.210
F(000)	704.0	704.0	704.0
Crystal size/mm^3	0.398 × 0.3 × 0.254	0.398 × 0.3 × 0.254	0.178 × 0.123 × 0.09
Radiation	MoKα (λ = 0.71073)	MoKα (λ = 0.71073)	MoKα (λ = 0.71073)
2Θ range for data collection/°	4.002 to 61.1	4.038 to 53.126	3.998 to 45.03
Index ranges	$-12 \le h \le 14$, $-19 \le k \le 16$, $-16 \le l \le 16$	$-13 \le h \le 13$, $-17 \le k \le 17$, $-14 \le l \le 14$	$-11 \le h \le 11$, $-14 \le k \le 15$, $-11 \le l \le 12$
Reflections collected	24994	17973	17901
Independent reflections	4866 [R_{int} = 0.0324, R_{sigma} = 0.0266]	3260 [R_{int} = 0.0398, R_{sigma} = 0.0290]	2085 [R_{int} = 0.0780, R_{sigma} = 0.0429]
Data/restraints/parameters	4866/486/254	3260/485/254	2085/485/254

Goodness-of-fit on F^2	1.027	1.091	1.062
Final R indexes [I>=2σ (I)]	R_1 = 0.0361, wR_2 = 0.0862	R_1 = 0.0359, wR_2 = 0.0783	R_1 = 0.0358, wR_2 = 0.0709
Final R indexes [all data]	R_1 = 0.0475, wR_2 = 0.0924	R_1 = 0.0465, wR_2 = 0.0825	R_1 = 0.0611, wR_2 = 0.0795
Largest diff. peak/hole / e $Å^{-3}$	0.39/-0.27	0.22/-0.21	0.17/-0.18

Table S2. Crystal data tables of (*Z*)**-HTI-An** at 298K, (*Z'*)**-HTI-An** at 400K.

Compound	(*Z*)**-HTI-An**	(*Z'*)**-HTI-An**
CCDC No.	2068877	2068878
Empirical formula	$C_{23}H_{14}OS$	$C_{23}H_{14}OS$
Formula weight	338.40	338.40
Temperature/K	**298**	**400**
Crystal system	monoclinic	monoclinic
Space group	$P2_1/c$	$P2_1/c$
a/Å	12.9474(18)	13.183(11)
b/Å	11.1005(17)	11.272(8)
c/Å	11.7019(17)	11.792(8)
α/°	90	90
β/°	97.279(5)	97.60(3)
γ/°	90	90

Volume/Å^3	1668.3(4)	1737(2)
Z	4	4
ρ_{calc}g/cm^3	1.347	1.294
μ/mm^{-1}	0.201	0.193
F(000)	704.0	704.0
Crystal size/mm^3	0.399 × 0.211 × 0.111	0.399 × 0.211 × 0.111
Radiation	MoKα (λ = 0.71073)	MoKα (λ = 0.71073)
2Θ range for data collection/°	3.172 to 52.824	3.116 to 53.81
Index ranges	-14 ≤ h ≤ 16, -13 ≤ k ≤ 11, -14 ≤ l ≤ 14	-16 ≤ h ≤ 16, -14 ≤ k ≤ 13, -14 ≤ l ≤ 14
Reflections collected	22309	18361
Independent reflections	3417 [R_{int} = 0.0323, R_{sigma} = 0.0255]	3576 [R_{int} = 0.0512, R_{sigma} = 0.0482]
Data/restraints/parameters	3417/0/226	3576/0/226
Goodness-of-fit on F^2	1.027	1.010
Final R indexes [I>=2σ (I)]	R_1 = 0.0365, wR_2 = 0.0840	R_1 = 0.0437, wR_2 = 0.0934
Final R indexes [all data]	R_1 = 0.0593, wR_2 = 0.0967	R_1 = 0.1038, wR_2 = 0.1183
Largest diff. peak/hole / e Å^{-3}	0.19/-0.22	0.14/-0.18

Table S3. Change in unit cell parameters of (*Z*)-**HTI-An** at 298 K and 400 K.

Unit Cell	(*Z*)-**HTI-An** at 298K	(*Z'*)-**HTI-An** at 400K	Expansion (%)
a (Å)	12.9474(18)	13.183(11)	1.82

b (Å)	11.1005(17)	11.272(8)	1.54
c (Å)	11.7019(17)	11.792(8)	0.77
Volume (Å^3)	1668.3(4)	1737(2)	4.24

Figure S10. Face indexing of (*Z*)-**HTI-An**.

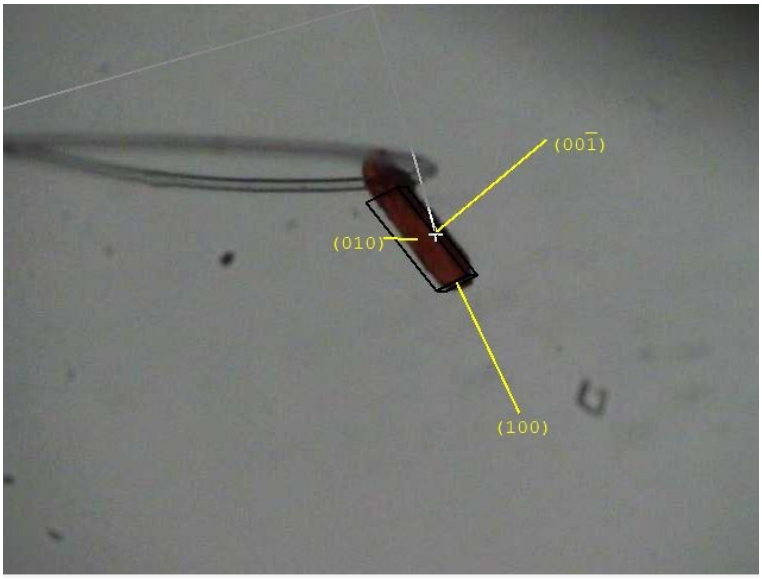

Figure S11. Face indexing of (*E*)-**HTI-An**.

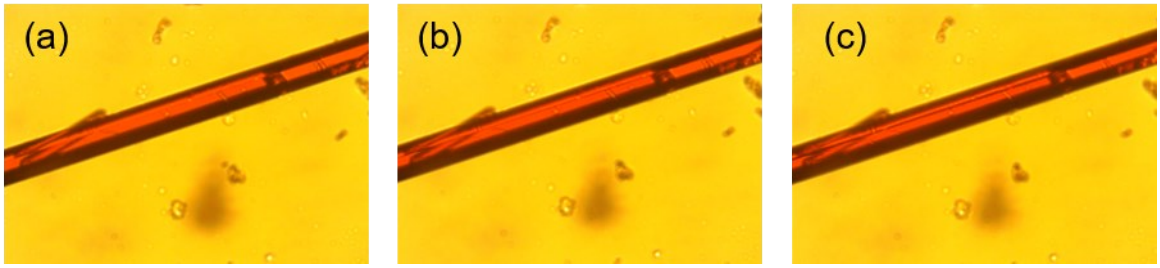

Figure S12. Slow heating of single crystal of (Z)-**HTI-An** induces a phase transition resulting in cracking along (001) plane.

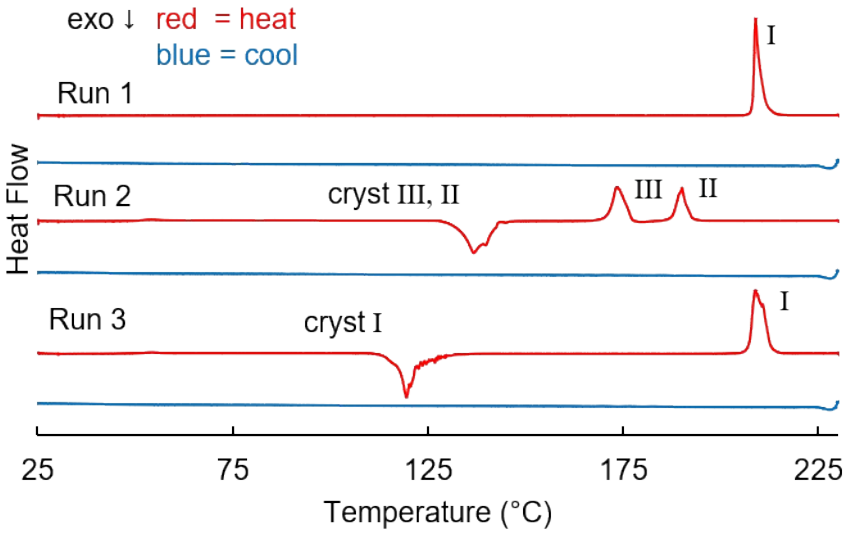

Figure S13. DSC heating/cooling runs beginning with crystalline (*Z*)-**HTI-An**. Run 1 shows the melting point of (*Z*)-**HTI-An** (**I**). Run 2 shows both crystallization and melting of two distinct new phases. Run 3 shows the recrystallization and remelting of phase **I** (*Z*)-**HTI-An**.

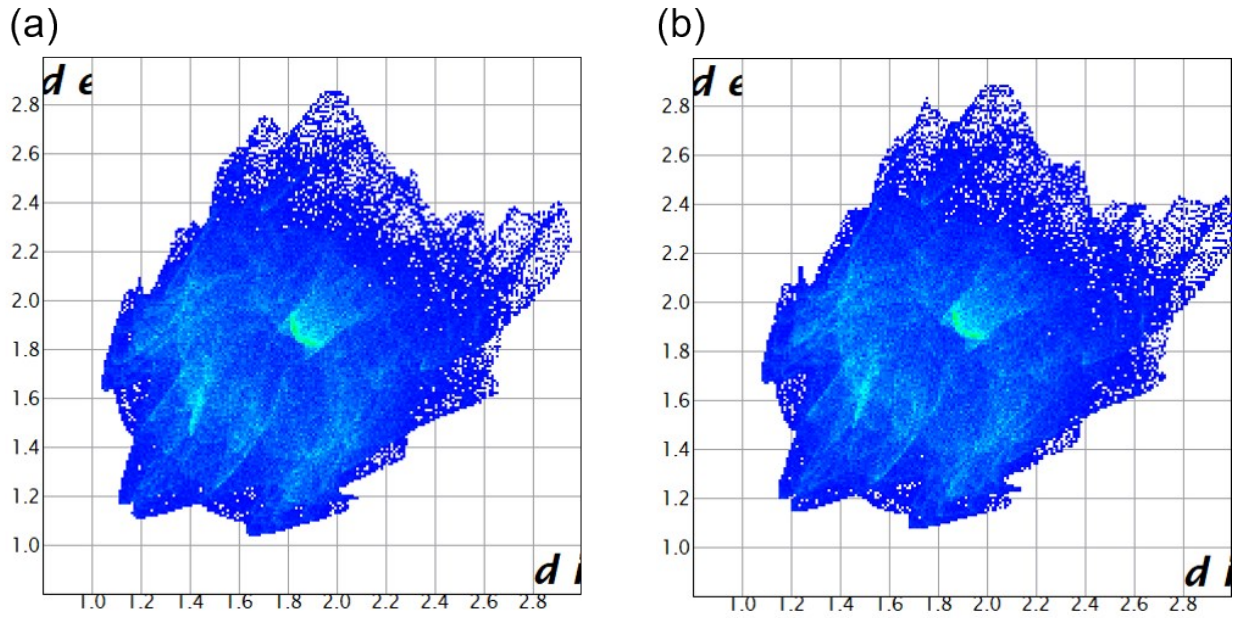

Figure S14. 2D Hirshfeld fingerprint plots of (a) (*Z*)-**HTI-An** and (b) (*Z'*)-**HTI-An**.

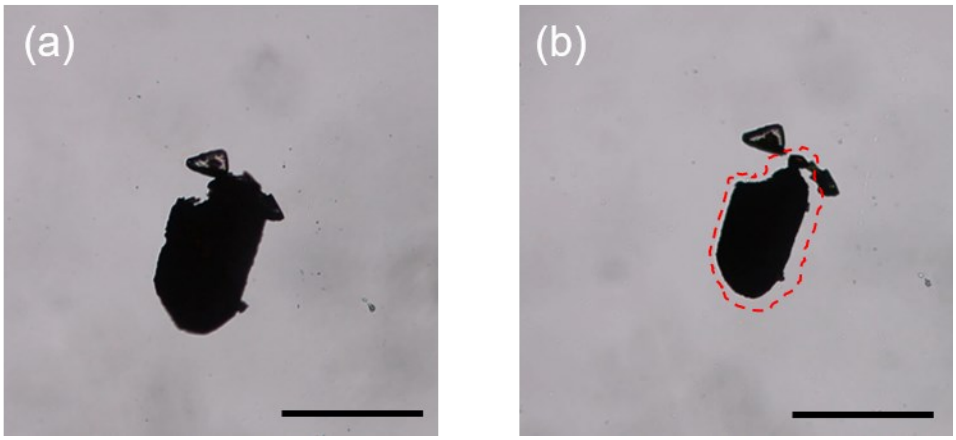

Figure S15. Crystal size reduction during thermal reversion of (*E*)-**HTI-An** at 180 °C for 2 hours. Scale bars are 200 μm.